Review article **Open Access**

Danqing Lu, Lei He, Ge Zhang, Aiping Lv, Ruowen Wang, Xiaobing Zhang and Weihong Tan*

Aptamer-assembled nanomaterials for fluorescent sensing and imaging

DOI 10.1515/nanoph-2015-0145
Received November 22, 2015; revised February 29, 2016; accepted March 17, 2016

Abstract: Aptamers, which are selected *in vitro* by a technology known as the systematic evolution of ligands by exponential enrichment (SELEX), represent a crucial recognition element in molecular sensing. With advantages such as good biocompatibility, facile functionalization, and special optical and physical properties, various nanomaterials can protect aptamers from enzymatic degradation and nonspecific binding in living systems and thus provide a preeminent platform for biochemical applications. Coupling aptamers with various nanomaterials offers many opportunities for developing highly sensitive and selective sensing systems. Here, we focus on the recent applications of aptamer-assembled nanomaterials in fluorescent sensing and imaging. Different types of nanomaterials are examined along with their advantages and disadvantages. Finally, we look toward the future of aptamer-assembled nanomaterials.

***Corresponding author: Weihong Tan,** Molecular Sciences and Biomedicine Laboratory, State Key Laboratory for Chemo/Biosensing and Chemometrics, College of Chemistry and Chemical Engineering, Collaborative Innovation Center for Chemistry and Molecular Medicine, Hunan University, Changsha 410082, China; and Department of Chemistry and Department of Physiology and Functional Genomics, Center for Research at the Bio/Nano Interface, Health Cancer Center, University of Florida, Gainesville, FL 32611-7200, USA, e-mail: tan@chem.ufl.edu
Danqing Lu, Lei He, Ge Zhang, Ruowen Wang and Xiaobing Zhang: Molecular Sciences and Biomedicine Laboratory, State Key Laboratory for Chemo/Biosensing and Chemometrics, College of Chemistry and Chemical Engineering, Collaborative Innovation Center for Chemistry and Molecular Medicine, Hunan University, Changsha 410082, China
Aiping Lv: Institute for Advancing Translational Medicine in Bone and Joint Diseases, School of Chinese Medicine, Hong Kong Baptist University, Hong Kong, China

Edited by Volker Sorger

Keywords: aptamer; bioimaging; biosensing; cancer therapy; disease diagnosis; drug delivery; nanomaterials; self-assembly.

1 Introduction

Fluorescent biosensing is a powerful tool for detecting biologically relevant morphological details as well as monitoring various physiological processes in living systems. It is noninvasive, highly sensitive, and disposed to fast analysis with spatial resolution. As such, fluorescent biosensing provides a promising approach to the early diagnosis of serious diseases as well as *in vivo* quantitative monitoring of drug release, and many biological targets have been identified across a wide spectrum of biosciences.

Aptamers are short single-stranded oligonucleotides (DNA or RNA) selected from 10^{12} to 10^{15} combinatorial oligonucleotide libraries *in vitro* by the systematic evolution of ligands by exponential enrichment (SELEX) process. By folding into distinct secondary or tertiary structures, aptamers can bind to a variety of targets, including peptides, proteins, drugs, organic and inorganic molecules, whole cells, or even tissues, with high affinity and specificity [1]. Since aptamers were first reported by the Szostak and Gold groups, respectively, in 1990 [2, 3], they have garnered considerable interest as a novel kind of recognition element in sensing systems based on their unique features, including (1) high affinity with equilibrium dissociation constants (K_d) from picomolar to micromolar, which are equal to or better than those of antibody-antigen complexes; (2) ability to bind discrete targets with high specificity [4]; (3) easy synthesis with the potential for adding functional groups; (4) wide range of targets from small metal ions to entire cells or pathogens; and (5) relatively high chemical stability even after storage for 1 year.

Nanomaterials, defined as having a size <100 nm in at least one dimension, also possess valuable properties, including good biocompatibility, facile synthesis and surface modification, and large surface area-to-volume ratio. By the effects of their surface volume and quantum

size, nanomaterials also exhibit unique optical, magnetic, and electronic properties. For example, compared to organic quenchers, gold nanoparticles (AuNPs), known as "superquenchers", provide more efficient fluorescent detection of DNA with 100-fold better sensitivity [5]. Based on these properties, carbon and gold nanomaterials, as well as quantum dots (QDs) and silicon nanoparticles, have gained increasing attention both in the construction of new fluorescent biosensors and in the delivery of nucleic acid probes into living cells for bioimaging applications [6].

By conjugating aptamers with nanomaterials, both specific molecular recognition and strong signal transduction can be achieved. With the large surface area-to-volume ratio, nanomaterials can carry a high aptamer payload, thus enhancing the sensing signal by several 1000-fold [7] and improving target recognition performance via cooperative interaction. Moreover, the integration of aptamers with nanomaterials protects aptamers from enzymatic degradation and nonspecific binding in the biological environment, thereby increasing the application of aptamer-assembled nanomaterials in cellular sensing and imaging.

In this review, we focus on recent advancements in the development of aptamer-assembled nanomaterials, including gold nanomaterials, carbon nanomaterials, QDs, silica nanoparticles, and DNA self-assembled nanostructures, all in the context of fluorescent sensing and imaging. We summarize the advantages and disadvantages of each kind of nanomaterial and the potential applications of aptamer-nanomaterial conjugates in bioanalysis and bioimaging.

2 Aptamer-assembled carbon nanomaterials for fluorescent sensing and imaging

Carbon is abundant in living systems, and by its dimensionality, carbon nanocrystals form (1) carbon composites (quasi-3D geometry), (2) graphene and graphdiyne (2D geometry), (3) carbon nanotubes (CNTs; 1D geometry), and (4) carbon QDs (CQDs), fullerene (0D geometry). In this review, we highlight graphene/graphene oxide (GO), CNTs, and CQDs for biochemical sensing and imaging applications based on their fluorescent properties or fluorescence quenching properties.

2.1 Graphene/GO

Graphene is a single-atom-thick planar sheet of sp^2-hybridized carbon atoms with 2D nanostructure and large specific surface area. Because of its unique structures and remarkable electrical, optical, and chemical properties, graphene has been broadly studied. GO, a water-soluble derivative of graphene, is a carbon structure predominantly decorated by a range of oxygen functional groups (e.g. carboxyl, hydroxyl, carbonyl, and epoxy groups), imparting a substantial degree of sp^3 hybridization. The fluorescence of GO ranges from ultraviolet (UV) to near-infrared (NIR) [8, 9] and can be enhanced by the modification with organic dyes or alkylamines [10, 11]. However, in bioanalysis, GO is more often considered as a highly efficient fluorescence quenching material. Based on fluorescence resonance energy transfer (FRET), fluorescently tagged probes, especially aptamers, attach firmly onto GO through strong π-π stacking, and the close interaction leads to fluorescence quenching. The distance between probes and GO is always <10 nm for FRET, whereas quenching is attainable even at a distance of 30 nm by GO [12]. Ever since the first isolation of free-standing graphene sheets in 2004 [13], graphene/GO have been successfully used in many biochemical applications, such as DNA analysis, enzyme activity analysis, protein assays, and drug delivery [14].

As shown in Figure 1, single-stranded DNA (ssDNA) can noncovalently bind with GO via nucleobases and aromatic compounds [15]. As a proof, atomic force microscopy (AFM) imaging showed that the fluorescence anisotropy of free ssDNA is 0.06, whereas that for

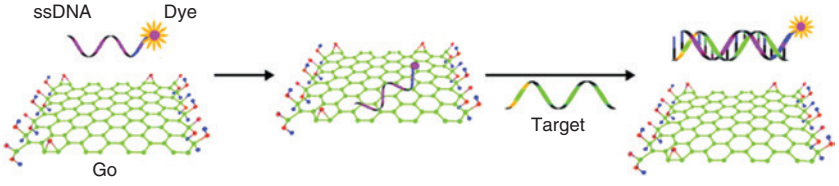

Figure 1: Schematic representation of target-induced fluorescence change of ssDNA-FAM-GO complex. Reprinted with permission of Ref. [15]. © Copyright 2009 Wiley-VCH Verlag GmbH & Co. KGaA.

the ssDNA-GO complex is 0.158. At the same time, 97% fluorescence of dye-labeled ssDNA was quenched by GO. Based on this research, human thrombin was sensitively and selectively detected by the use of dye-labeled human thrombin aptamer and GO [16]. A logical sensing platform of multiplex targets was constructed by Wang et al. In this work, ATP aptamer and human thrombin aptamer were adsorbed onto GO with different dye labels. In the presence of ATP or thrombin, the conformational change between target and aptamer led to fluorescence recovery of the labeled dye [17].

Adopting a similar design, many analytes able to specifically bind with aptamers were detected, including silver(I) (Ag) ions [18], insulin [19], ochratoxin A [20], and human thrombin [15]. It is worth mentioning that intracellular ATP was recognized and imaged *in situ* by this strategy [21].

Aptamer-GO conjugates afford many advantages. First, apart from its electronic and optical properties, GO also shows excellent water solubility and biocompatibility in living systems. Moreover, compared to single-walled CNTs (SWCNTs), GO is less cytotoxic. Second, the strong binding between aptamer and GO decreases enzymatic cleavage and nonspecific aptamer binding and hence increases selectivity and sensitivity. Third, based on smart design, intercellular/intracellular real-time monitoring and imaging of target can be achieved in a simple, cost-effective way.

2.2 CNTs

CNTs are mosaics of carbon atoms that form graphene sheets and curl into seamless tubules [22]. Specifically, whereas SWCNTs are characterized by walls formed by one-atom-thick sheets of carbon (or graphene), multi-walled CNTs (MWCNTs) will have a layer of many such sheets. In general, CNTs, a member of the fullerene structural family, have demonstrated interesting physicochemical, electrical, and mechanical properties. In particular, SWCNTs exhibit fluorescence emission and quenching properties in the NIR range, supplying very low background signal in living systems. When SWCNTs are aggregated into bundles, fluorescence emission disappears, whereas absorption spectra are correspondingly broadened. These fluorescent properties promote SWCNTs as powerful candidates for biosensing and bioimaging.

Different from graphene, CNTs are quasi-1D nanostructures with distinct inner and outer surfaces. The inner space of CNTs can be loaded with materials ranging from anticancer drugs to dyes, whereas the outer surface can be assembled with aptamers. Furthermore, the noodle-like shape of CNTs permits their entry into the cell membrane via endocytosis without any requirement for external transport systems [23, 24]. Based on fluorescence emission, CNTs can act as a reporter in the construction of biosensors. For example, based on fluorescence by the dissolution and aggregation of CNTs, a label- and separation-free NIR optical method was designed for protein detection [25].

On the contrary, because the absorption spectrum of CNTs spans a wide range of wavelengths (approximately 500–900 nm), CNTs can act as an acceptor in FRET, whereas various fluorophores can act as a donor. Dye-labeled ssDNA, which wrapped on SWCNTs by means of π-stacking interactions, resulted in fluorescence quenching. However, after the addition of the complementary DNA strand, dye-labeled ssDNA was separated from SWCNTs, increasing fluorescence [26]. By employing an aptamer molecule as a recognition element, different targets, such as human α-thrombin (Tmb) [26], lysozyme (LYS) [27], and cancer cells [28], can be sensed. For instance, Yan et al. assembled Cy5-labeled sgc8c aptamer on SWCNTs to construct an activatable fluorescence probing platform (Cy5-sgc8c/SWCNT complex). sgc8c aptamer, as the recognition element, specifically binds to CCRF-CEM cancer cells. In the presence of target, sgc8c aptamer, but not SWCNTs, bound to the target cell, as effectively reported by fluorescence enhancement of the Cy5 dye. Therefore, CCRF-CEM cancer cells could be clearly imaged as a result of aptamer binding both *in vitro* and *in vivo* [28].

Apart from their optical properties, aptamer-modified CNTs, as an emerging drug carrier, have been demonstrated to protect aptamers from enzymatic digestion or degradation. Finally, a novel photodynamic therapy (PDT) was selectively triggered by building an aptamer-photosensitizer-SWCNT complex. The ssDNA aptamer was protected by SWCNT from enzymatic digestion or degradation, and singlet-oxygen generation (SOG) was controllably released after aptamer-target binding [29].

In summary, SWCNTs furnish a multifunctional platform for aptamer-based sensing and imaging. Based on the fluorescence emission and universal fluorescent quenching properties of CNTs, the aptamer-CNT complex probe provides low background and high signal-to-noise ratio for increased sensitivity. Based on the large surface area and relatively weak adsorption, CNTs can be loaded with multiple aptamers for multiplexed sensing and, at the same time, protect aptamers from enzymatic degradation and nonspecific binding for high selectivity. However, the toxicity of CNTs is still contentious. To obtain considerable and accurate experimental data in sensing and

imaging, more standard and reliable detection methods should be established.

2.3 CQDs

CQDs, also known as "graphene QDs (GQDs)" or "carbon dots (CDs or C-Dots)", were accidentally discovered in 2004 during the separation and purification of SWCNTs [30]. Ever since the discovery of CQDs, their underlying mechanism of fluorescence emission has been debated. One theory holds that bandgap transitions are caused by conjugated π-domains. It is also conjectured that the mechanism involves surface defects in CQDs. Irrespective of which theory is correct, fluorescence emissions of CQDs cover a broad range of the visible region and extend into the NIR region. As shown in Figure 2, CQDs show tunable fluorescence emissions that are excitation wavelength dependent [31]. Moreover, the fluorescence of CQDs is notably enhanced by surface passivation.

The fluorescent properties of CQDs have been broadly studied in fluorescent sensing and imaging. For example, Qian et al. demonstrated an "on-off-on" process to detect lead(II) ion (Pb^{2+}) with a detection limit of 0.6 nM. The aptamer-CQDs were mixed with GO to quench the fluorescence of CQDs via electrostatic attraction and π-π stacking interaction. An aptamer specific to Pb^{2+} was covalently cross-linked to CQDs. Upon the addition of Pb^{2+}, the aptamer formed a G-quartet with Pb^{2+}, and the aptamer-CQDs complex separated from GO. As a result, fluorescence was recovered [32]. CQDs have also been exploited as an energy acceptor whereby up-converting phosphors (UCPs) acted as the energy donor to build a FRET sensor for thrombin [33]. By changing the energy donor from UCPs into Mn-doped ZnS QDs (Mn-ZnS QDs), thrombin was then sensed owing to phosphorescence energy transfer (PET) between Mn-ZnS QDs and CQDs [34].

Similar to some carbon materials, such as CNTs, dispersion and aggregation can lead to fluorescent changes for CQD. Mucin 1 (MUC1) was detected by the immunoreaction between CQD-labeled antibody and the CQD-labeled aptamer. The absence and presence of MUC1 led to the dispersion and aggregation of CQDs, and fluorescent changes were the response [35]. In addition to conventional down-conversion fluorescence, CQDs reveal up-conversion fluorescence as well [36]. Cho et al. synthesized up-converted CQDs and detected copper(II) ion (Cu^{2+}) with high sensitivity and selectivity via aptamer-mediated Cu^{2+} metal ion detection by taking advantage of up-converted CQDs [37].

Apart from their role as fluorescent emitters, CQDs can also act as a nanoquencher of chromophores or dyes based on electrostatic repulsion and π-π stacking interactions. As a demonstration, CQDs quenched the fluorescence of dyes as the dye-labeled ATP aptamer strongly bound to CQDs. The addition of ATP competitively bound to aptamer and caused fluorescence recovery [38].

Although traditional semiconductor QDs have remarkable optical properties, they also have some shortcomings, such as biological toxicity, poor water solubility, and "blinking" behavior. To address these limitations, CQDs have shown low toxicity, excellent biocompatibility, adequate water solubility, good resistance to photobleaching, and stable emission. Owing to these superior properties, CQDs are playing a critical role in analytical and bioanalytical science. Unfortunately, CQDs with high quantum yields remain rare.

3 Aptamer-assembled gold nanomaterials for fluorescent sensing and imaging

Over the last two decades, gold nanomaterials have attracted wide interest because of their unique optical, electronic, and chemical properties. By changing the parameters during synthesis, gold nanomaterials can be

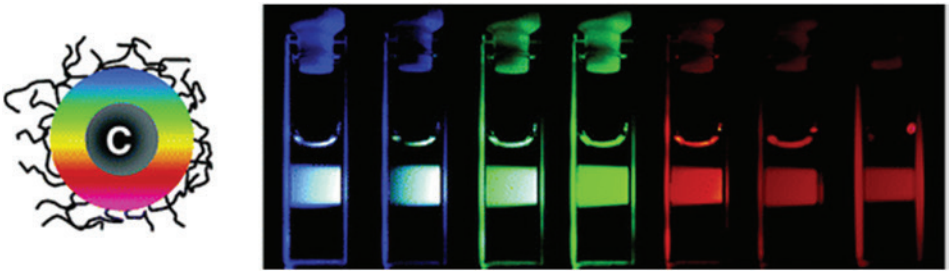

Figure 2: Aqueous solution of PEG1500N-attached carbon dots. Reprinted with permission of Ref. [31]. © Copyright 2006 American Chemical Society.

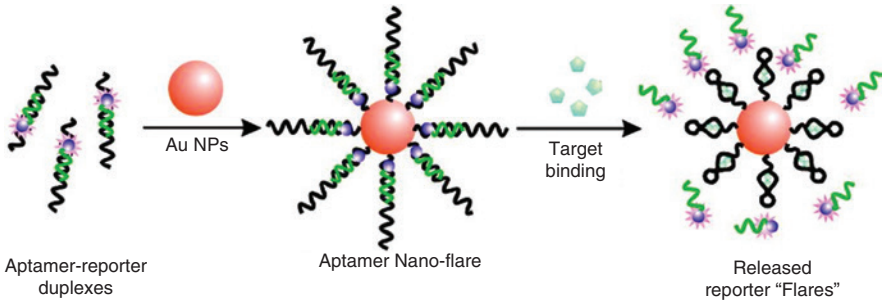

Figure 3: Aptamer nanoflares are AuNPs functionalized with thiol-terminated aptamer sequences hybridized to a short complementary Cy5-labeled reporter strand. The reporter was displaced when the presence of target molecule induced a conformational change of the aptamer. Reprinted with permission of Ref. [40]. © Copyright 2009 American Chemical Society.

synthesized in diverse sizes and shapes, such as AuNPs, gold nanorods (AuNRs), and gold nanoclusters (AuNCs).

3.1 AuNPs

Based on efficient energy/charge transfer, AuNPs always exhibit superquenching of fluorescence toward either organic dyes or other luminescent nanoparticles. For example, the fluorescent quenching between AuNPs and cationic-conjugated polymers is 9–10 orders of magnitude more efficient than that of typical small-molecule dye-quencher pairs [39]. To date, AuNPs have been broadly used as signal reporters in fluorescent sensing and imaging systems.

Using an aptamer-AuNP composite probe, termed aptamer nanoflare, Mirkin's group has detected and quantified a small-molecule analyte in the living cell. As shown in Figure 3, Cy5-labeled reporter strands acting as flares were hybridized with ATP aptamers, which were covalently attached to the surface of AuNPs via Au-thiol bond, thereby quenching the fluorescence of flare strands by AuNPs. In the presence of ATP, the fluorescence signal recovered essentially because ATP-aptamer interaction induced a conformational change of the aptamer, resulting in greater separation between the flares and gold surface [40]. Such aptamer nanoflares can be extended to simultaneously detect multiple analytes in homogeneous solution. Fan et al. assembled three kinds of 3′-thiolated complementary DNA strands on the surface of AuNPs. Each strand could hybridize an aptamer labeled with a specific dye at the 5′-end. As a result of energy transfer, the fluorescence of all three dyes was quenched. The presence of specific targets would significantly change the conformation of the corresponding aptamer, causing the aptamer to separate from the AuNPs surface and hence recovering fluorescence of the corresponding labeled dye. This aptamer-based multicolor gold nanoprobe has been developed for simultaneous detection of adenosine, potassium, and cocaine [41]. Moreover, these aptamer-AuNP conjugates can be used to detect small molecules and metal ions and to measure the distance between two binding sites on a cell membrane receptor via a surface energy transfer (SET) nanoruler. For example, Chen et al. have successfully measured the distance between the binding sites of aptamer and antibody on tyrosine-protein kinase-like 7 (PTK7), a transducer of extracellular signals across the cell membrane, in the lipid bilayer of the CEM cell membrane, by employing sgc8 aptamer, which specifically recognizes PTK7, to form an sgc8 aptamer-AuNP conjugate and organic dye-labeled anti-PKT7 as an SET nanoruler [42].

3.2 AuNRs

Anisotropic AuNRs can be tuned with aspect ratios (length/diameter), and their absorption spectra present two surface plasmon resonance bands: one for the transverse (short axis) plasmon and the other for the longitudinal (long axis) plasmon [43]. Their distinctive surface plasmon resonance bands span from the UV to NIR region and enable AuNRs to efficiently convert the absorbed radiation into heat and even kill living cells, i.e. AuNRs can act as hyperthermia agents for photothermal therapy (PTT). In particular, PTT/PDT was used for a novel dual-therapy strategy employing AuNRs as hyperthermia agents and Ce6 as photosensitizers. Aptamer sgc8 conjugated on the surface of AuNRs was then hybridized with a Ce6-labeled ssDNA to form a DNA double helix. In the presence of target cells, the aptamers would preferentially bind to the target cells and release the Ce6-labeled ssDNA. Upon light irradiation, Ce6 produced singlet oxygen for PDT, and AuNRs produced heat for PTT [44]. Although promising, hyperthermia agents for PTT still suffer some problems in biochemical applications. Specifically, the dispersion and

morphological control of AuNRs are commonly assisted by various surfactants such as cetyltrimethylammonium bromide (CTAB), but these surfactants are usually cytotoxic and thus have limited applications in living cells.

3.3 AuNCs

AuNPs and AuNRs are widely considered to be superquenchers to efficiently quench the fluorescence of a broad range of dyes through energy/charge transfer processes [45, 46]. On the contrary, the AuNCs composed of a few to about 100 gold atoms with a size smaller than 2 nm have strong photoluminescence features with large Stokes shift and excellent photostability. The luminescent AuNCs provide the missing link between atomic and nanoparticle behaviors in noble metals [47] and show high potential in biochemical applications. The Yan group reported a competitive method for sensitive and selective detection of ATP using AuNCs. T-rich ssDNA binding with Hg^{2+} to form a T-Hg-T hairpin structure acted as the complementary sequence of the ATP aptamer. In the absence of ATP, the ATP aptamer competed with Hg^{2+} to hybridize with the ssDNA, leading to the release of Hg^{2+}. The energy transfer between AuNCs and Hg^{2+} caused fluorescence quenching. However, in the presence of ATP, ATP aptamers folded into a secondary structure so that the T-Hg-T structure failed to open, which produced strong fluorescence to realize sensitive and selective detection of ATP [48].

Apart from AuNPs, AuNRs, and AuNCs, gold-coated nanomaterials have also been employed as multifunctional nanomaterials, e.g. iron oxide (Fe_3O_4@Au) nanoroses. By constructing aptamer-modified Fe_3O_4@Au nanoroses and intercalating DOX in the modified DNA sequences, this aptamer-conjugated Fe_3O_4@Au platform exhibited five distinct functions for simultaneous imaging and therapy: targeting with aptamers, dual molecular imaging [magnetic resonance imaging (MRI)/optical imaging], and dual therapy (photothermal/chemotherapy) [49].

In sum, AuNPs, AuNRs, and AuNCs, as well as gold-coated nanomaterials, have been synthesized and modified with aptamers, resulting in high intracellular stability, high DNA-loading capacity, and easy surface modification in biochemical applications.

4 Aptamer-assembled QDs for fluorescent sensing and imaging

QDs are quasi-0D nanoparticles ranging from 2 to 10 nm in diameter. Compared to organic fluorophores and dyes, QDs have exceptional optical properties, including (1) high fluorescence quantum yields, (2) long fluorescence lifetimes, (3) high stability against degradation and photobleaching, (4) narrow fluorescence emission spectra, and (5) large Stokes shifts. Additionally, the controllable size and shape of QDs afford absorption and emission spectra ranging from UV to NIR bands. These features are crucial for ultrasensitive detection and real-time tracking and monitoring of complex biological events. Combined with aptamers, QDs have been widely applied in fluorescent sensing and imaging.

In general, the fluorescence of QDs is quenched by either FRET or chemiluminescence resonance energy transfer (CRET). The Ellington group reported the first sensor based on the thrombin aptamer-QDs complex, in which a complementary quencher-labeled DNA strand of thrombin aptamer was hybridized. The presence of thrombin, as detected by aptamer-specific ligation, resulted in the release of the quencher-labeled strand, thereby recovering fluorescence [50]. Similarly, a series of sensing platforms for vascular endothelial growth factor (VEGF) were designed using QDs as a fluorescent signal reporter

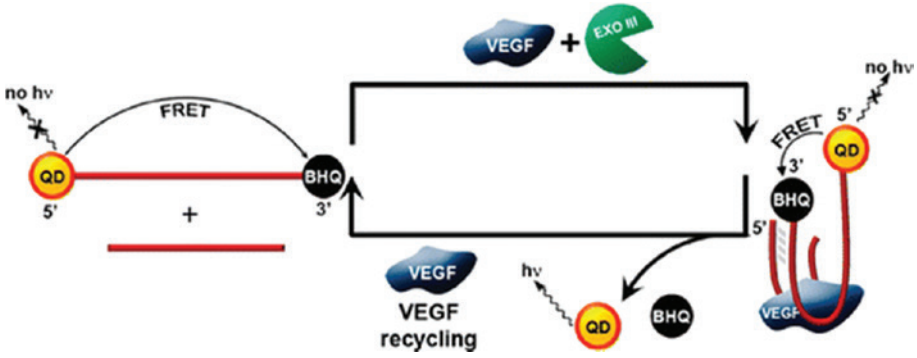

Figure 4: FRET analysis of VEGF165 by anti-VEGF aptamer-modified CdSe/ZnS QDs. Reprinted with permission of Ref. [51]. © Copyright 2012 American Chemical Society.

(Figure 4). FRET-based sensors, the chemiluminescence aptasensor, and the CRET-based aptasensor were designed to construct sensing platforms for VEGF, as it is an important biomarker in cancer research [51]. QDs were synthesized and conjugated with aptamer AS1411 to form an aptamer-QD complex. Because nucleolin, the target of AS1411, is overexpressed in cancer cells, the fluorescence imaging of cancer cells was achieved [52]. A multicomponent sensing system for the simultaneous detection of adenosine and cocaine was designed using QDs as a fluorescence quencher to encode aptamer-linked nanostructures. The analytes were detected and quantified in one pot by following the changes in color and fluorescence [53].

QDs are nanocrystals made of semiconductor materials, i.e. nanoparticles with sizes from hundreds to thousands of atoms of groups II and VI elements (e.g. CdSe and CdTe) or groups III and V elements (e.g. InP and InAs) [54]. However, heavy metal elements, such as Cd, are toxic and harmful to living systems. To broaden the QD family and optimize their performance, other kinds of QDs are under development, including carbon QDs with the advantages of low toxicity, environmental safety, low cost, and simple synthetic routes.

5 Aptamer-assembled silica nanoparticles for fluorescent sensing and imaging

Despite the absence of fluorescent properties, silica nanoparticles offer a promising platform for biosensing and bioimaging [55]. Interestingly, by doping organic dyes or using templates in the synthesis process, modified silica nanoparticles stand out as superior nanovectors by their high capacity, demonstrated cargo protection, universal biocompatibility, easy separation, and facile functionalization.

5.1 Mesoporous silica nanoparticles (MSNPs)

With such templates as CTAB available in the synthesis process, MSNPs can be synthesized. These unique hollow structures are endowed with high surface areas, stable and rigid frameworks, tunable pore sizes, and large pore volumes. Meanwhile, the high surface area-to-volume ratio makes it easy to introduce various organic functional groups through either covalent bonding or electrostatic interactions. Different types of cargo molecules can be encapsulated into the pore channels simultaneously with complete protection from outside interference. The loaded cargo molecules can be released by control over the opening and closing of pore channels. Also, MSNPs are easily separated from solution by centrifugation. As a result, MSNPs have been extensively studied as nanocarriers for molecular sensing, cellular imaging, and drug delivery.

Hou et al. loaded glucose in MSNPs as reporter for nonglucose target detection by glucometer readout. Aptamers were hybridized with DNA1 grafted on the outer surface of the MSNPs and DNA2 labeled on AuNPs. Thus, a three-stranded complex, including MSNPs and AuNPs, formed and the pores were gated by AuNPs. By entrapping the glucose molecules inside MSNPs, targets could be read by glucometer, as the target-aptamer interaction separated AuNPs from MSNPs, leading to the release of glucose [56]. Also, a vitamin-responsive MSNPs nanocarrier was constructed with DNA aptamers. Doxorubicin (DOX), an ordinary anticancer drug, was loaded into aptamer-conjugated MSNPs with the pore channels capped by the desthiobiotin-avidin complex. DOX was capsulated in the pores before reaching the target cells. Vitamin H in target cells unlocked the capped desthiobiotin-avidin complex and enabled drug release to image and kill the cells [57]. Signal amplification detection and controlled drug release platforms were achieved. Because either signal reporter or anticancer drug was entrapped in MSNPs, the unlocking process was amplified by regeneration of the target-triggered mechanism [58].

5.2 Core-shell silica nanoparticles

Silica nanoparticles are chemically inert and resistant to many reagents. They always coat other substances and act as shells to protect the functional core. Core-shell nanoparticles, such as Fe_3O_4@SiO_2 [59] and QDs@SiO_2 [60], were synthesized to gain multifunctional nanostructures. For example, the QDs@SiO_2 complex combines fluorescence and mesoporous structure to achieve a targeting and tracking system. As shown in Figure 5, Zhang et al. fabricated a DNA hybrid-capped mesoporous silica-coated QD (MSQD) system. The MSQD substrate emitted strong fluorescence by the QD core and possessed notable photostability, owing to the protection by the silica shell. Because of the proton-sponge effect, some of MSQDs successfully escaped from the endosome/lysosome into the cytoplasm. The DNA hybrid consisted of AS1411 aptamer targeting cancer cells and miR-21 antisense oligonucleotides to

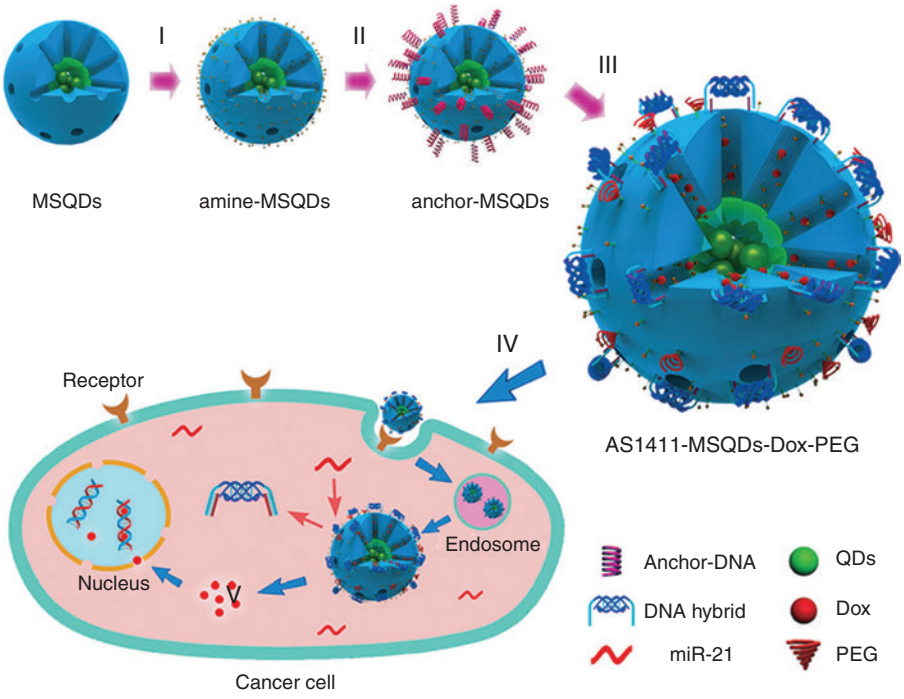

Figure 5: Preparation and application of miRNA-responsive controlled drug delivery nanocarriers. Reprinted with permission of Ref. [61].

control drug release. By capping the DNA hybrid to MSQDs after drug loading, the system was traceable with control over drug delivery [61].

During the formation of silica nanoparticles, a large number of dyes can be encapsulated inside each nanoparticle to produce dye-doped silica nanoparticles, i.e. dye-doped SiNPs. Compared to single-dye molecules, the luminescence of single dye-doped silica nanoparticles is approximately 10^4 times stronger [62]. Moreover, silica nanoparticles are "transparent" in the sense that they do not absorb light in the NIR, visible, or UV regions or interfere with magnetic fields. Dye molecules doped in silica nanoparticles have high photostability, as they are isolated from the active outside environment. Consequently, dye-doped SiNPs conjugated with aptamers have been demonstrated as excellent substrates for optical signaling in biosensing and bioimaging.

In a recent work, aptamers labeled with quenchers were covalently modified on dye-doped SiNPs. In the presence of thrombin, aptamer-thrombin interaction drew quenchers close to dye-doped SiNPs and led to fluorescence quenching [63]. For pathogen detection, aptamer-conjugated dye-doped SiNPs were used to amplify the fluorescent signal and reduce false-positive signals [64]. Beyond target sensing, aptamer-conjugated dye-doped SiNPs were developed for cell monitoring and imaging [65–67].

6 Aptamer-containing DNA self-assembled nanostructures for fluorescent sensing and imaging

DNA molecules can self-assemble via noncovalent bonds and disassemble as a result of environmental changes. By taking advantage of molecular self-assembly and disassembly, goals, such as cargo delivery, can be realized.

DNA plays a pivotal role in such processes as gene expression. Recently, DNA has been developed to design and produce various 1D, 2D, and 3D nanostructures with sophisticated morphologies based on increasingly mature nanotechnologies. By drawing on different functionalized molecules, these DNA nanostructures are potential candidates for disease diagnosis, cellular imaging, and drug delivery based on their high biocompatibility, excellent cell permeability, self-assembly/disassembly properties, and efficient cell internalization.

6.1 Aptamer micelle

Micelles are aggregates of amphipathic molecules that disperse in colloidal solution. Micelles self-assemble via hydrophobic interaction, electrostatic interaction,

or hydrogen bonding. By attaching a hydrophobic tail to the end of an aptamer, aptamers can self-assemble into aptamer micelles [68]. Similar to polymeric micelles, aptamer micelles possess a special core-shell structure, such that the inner core offers a large space for hydrophobic molecules. The dense packing of aptamers in one micelle creates a multivalent effect that increases the binding affinity of aptamers. Aptamer-micelles are therefore widely used in diagnosis, imaging, and drug delivery.

In 2009, the Tan group reported an efficient detection/delivery vehicle termed aptamer-micelle. They modified a hydrophobic tail to the end of TDO5 aptamer, which showed a high affinity and selectivity to Ramos cells at 4°C. The fabricated aptamer-micelle improved the binding abilities of the aptamer moiety at both 4°C and 37°C, although TDO5 aptamer did not bind with Ramos cells at physiological temperature. By doping a special dye, which only fluoresces inside cells, into micelles for real-time monitoring, fusion between micelles and cell membranes was demonstrated within minutes [69]. A diameter of several tens of nanometers allowed micelles to reside in blood circulation and accumulate in solid tumors. Most recently, a multifunctional composite micelle was exploited for *in vivo* real-time imaging and drug delivery. DOX was encapsulated into AS1411-modified micelles for cancer therapy. Compared to free DOX, this aptamer-micelle delivery system extended blood circulation time and enhanced antitumor efficacy [70].

Despite their favorable characteristics, the use of micelles is limited by the critical micelle concentration (CMC), which is defined as that concentration of surfactants, or detergents, above which micelles form, and additional surfactants added to the system will simply go to micelles. In other words, although surfactants are soluble in water, they will aggregate into micelles when a sufficient concentration is reached. Therefore, below the CMC, no micelles form, but above the CMC the number of micelles increases in proportion to the increasing concentration of surfactant. In this sense, CMC is a value that reports how easily a micelle can take shape.

6.2 Aptamer-containing hydrogel

Hydrogels are polymer networks extensively swollen with water. DNA hydrogels are created by physically entrapping DNA into hydrogel networks or covalently conjugating DNA to the polymer backbone. For example, Y-shaped DNA and aptamer linkers self-assembled into a DNA hydrogel by cross-linking hybridization. AuNPs were first entrapped in DNA hydrogels and acted as signal indicators. The presence of target led to the collapse of DNA hydrogels and release of AuNPs. The released AuNPs attracted the postadded QDs via electrostatic interaction and quenched fluorescence of QDs via FRET [71]. Because hydrogels respond to stimuli or targets undergoing structural changes, i.e. sol-to-gel and gel-to-sol transitions, visual sensors based on hydrogels have been successfully constructed [72].

6.3 Other aptamer-containing DNA nanostructures

Based on rolling circle replication (RCR), a novel method to generate a new kind of DNA nanostructure, termed metahydrogel [73] or microsponge [74], was recently reported. In this method, polymerase enzyme was used to elongate DNA chains and weave them noncovalently into DNA architectures. For example, the Tan group built a noncanonical self-assembled DNA nanostructure, termed DNA nanoflower (NF), for cancer cell recognition, bioimaging, and targeted drug delivery. As shown in Figure 6, the DNA NFs were assembled from elongated DNA strands that were generated via RCR of a designer template. By designing appropriate templates, the NFs contained a high density of functional units, for example, aptamers, for biomedical applications. These aptamer-containing NFs showed exceptional properties, including low toxicity; high-capacity encapsulation of aptamers and other functional moieties; forceful resistance to nuclease degradation, denaturation, or dissociation; and efficient delivery of cargoes [75]. Based on this design, aptamer-conjugated FRET-NFs were described for multiplexed imaging under one single-wavelength excitation and traceable targeted drug delivery [76]. In general, NFs have the advantages of easy synthesis and modification, simple design, controllable size, and possible multivalent effects. However, NFs are confined by the activity of polymerase enzyme during synthesis. In addition, the dense packaging of a great number of DNAs may lead to potential immunotoxicity.

Aptamer-containing DNA can also self-assemble into manifold nanostructures for fluorescent sensing and imaging. Introduced by Dirks and Pierce in 2004 [77], hybridization chain reaction (HCR) leads to a cascade of DNA hybridizations through the introduction of triggering sequences. Taking advantage of such triggering mechanism, HCR systems can self-assemble into linear structures or branched structures [78]. An aptamer-tethered DNA nanostructure, termed aptamer nanotrain, was developed based on HCR. As recognition moiety, an aptamer serves as the nanotrain's target-specific engine. Probes tethered on the aptamer trigger HCR, resulting in the formation of a long, linear, double-stranded DNA

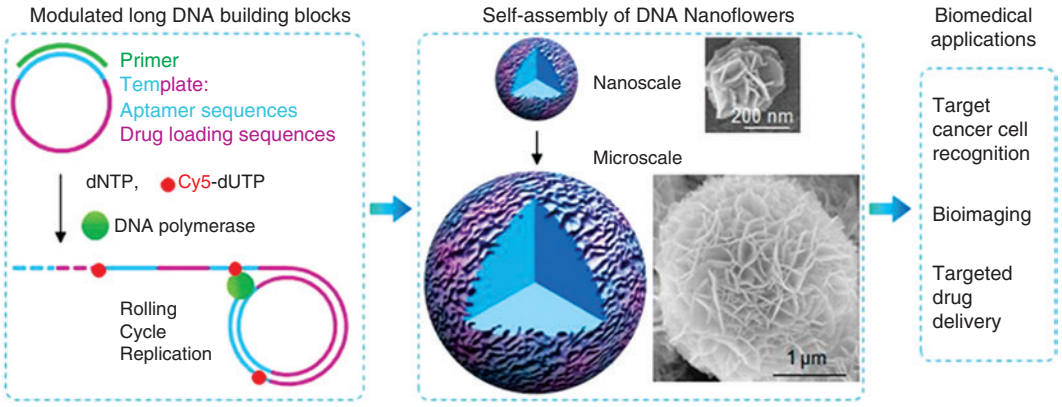

Figure 6: Schematic illustration of noncanonical self-assembly of multifunctional DNA NFs. Reprinted with permission of Ref. [75]. © Copyright 2013 American Chemical Society.

(dsDNA) nanostructure, the nanotrain proper consisting of a series of site-specific, cargo-bearing "boxcars." These "trailing" DNA boxcars are periodically aligned and supply a large number of spatially addressable sites, allowing high-capacity loading of anticancer drugs and bioimaging agents. The self-assembled aptamer nanotrain is an unprecedented advancement in bioimaging and targeted cancer therapy by *in vivo* real-time drug transport, *in vitro* cytotoxicity assay, and *in vivo* anticancer efficacy [79]. Extending this work, Zhu et al. physically assembled fluorophores into the boxcars or modified fluorophores on ssDNA monomers for HCR to form a FRET nanotrain. The FRET nanotrain demonstrated (1) selective anchoring and (2) *in situ* self-assembly on the target cell surface [80]. More than linear HCR structures, branched HCR structures also play an important role in biosensing and bioimaging. Taken together, DNA self-assembly nanostructures via HCR are easily constructed via enzyme-free synthesis.

Since DNA origami was first reported by Rothemund in 2006, different 2D and 3D DNA origami structures, such as squares, stars, tetrahedra, and truncated octahedra, have been constructed by different research groups [81–83]. Ke et al. used a rectangular-shaped origami structure for single-molecule detection of hybridization events [84]. An aptamer-containing DNA origami was also developed as a yeoman sensing system for biological detection. Yan's group carried out a label-free investigation of the effect of precisely controlled spacing between two ligands on the multivalent binding of a target protein [85].

7 Conclusion and outlook

In summary, aptamer-assembled nanomaterials have been used in a variety of sensing and imaging systems based on their superior properties. Their high binding sensitivity, high specificity, and simplicity of synthesis and modification, together with the wide range of targets and relatively high chemical stability, make aptamers key recognition elements. Meanwhile, the high biocompatibility, large surface area-to-volume ratio, facile surface modification, and overall structural robustness make nanomaterials ideal vehicles for aptamer delivery and protection. The resulting aptamer-nanomaterial conjugates show sensitive and selective molecular sensing as well as highly efficient delivery of reagents.

Nevertheless, some challenges remain. Up to 2012, only some 250 aptamers had been sequenced [86]. Hence, more kinds of aptamers need to be selected *in vitro* via SELEX technology. Also, tissues, blood, and water exhibit minimal absorption and autofluorescence in the NIR region. As a result, employing an NIR fluorescent signal for biosensing and imaging is critical for biomedical applications. Although the wavelength of the fluorescence emission of nanomaterials spans from the UV to NIR region, the fluorescent quantum yield of nanomaterials with NIR emissions remains unsatisfactory. Therefore, new materials and approaches are needed to improve fluorescent quantum yields in the NIR range. Furthermore, more efficient sensing systems with good biocompatibility need to be exploited for efficient detection of biological targets in complex sample matrices in clinical applications.

Acknowledgments: The authors would like to thank the members of the Molecular Science and Biomedicine Laboratory for helpful discussions related to this work. Specifically, we thank Liping Qiu, Honglin Liu, Liang Cui, Rong Hu, Lei Mei, Ding Ding, and Yongchao Liu for their help in writing this paper.

Funding: This work was supported by the National Key Scientific Program of China (2011CB911000), the National Key Basic Research Program of China (2013CB932702), NSFC (Grants 21325520, 21405100, 21405041, 21327009, 51302117, J1210040, and 21177036), the Foundation for Innovative Research Groups of NSFC (Grant 21221003), the National Instrumentation Program (2011YQ030124), and the Hunan Provincial Natural Science Foundation (Grant 11JJ1002).

References

[1] Liu J, Cao Z, Lu Y. Functional nucleic acid sensors. Chem Rev 2009;109:1948–98.
[2] Ellington AD, Szostak JW. In intro selection of RNA molecules that bind specific ligands. Nature 1990;346:818–22.
[3] Tuerk C, Gold L. Systematic evolution of ligands by exponential enrichment: RNA ligands to bacteriophage T4 DNA polymerase. Science 1990;249:505–10.
[4] Jenison RD, Gill SC, Pardi A, Polisky B. High-resolution molecular discrimination by RNA. Science 1994;263: 1425–29.
[5] Dubertret B, Calame M, Libchaber AJ. Single-mismatch detection using gold-quenched fluorescent oligonucleotides. Nat Biotechnol 2001;19:365–70.
[6] Kong R, Zhang X, Chen Z, Tan W. Aptamer-assembled nanomaterials for biosensing and biomedical applications. Small 2011;7:2428–36.
[7] Wang J. Nanomaterial-based amplified transduction of biomolecular interactions. Small 2005;1:1036–43.
[8] Sun X, Liu Z, Welsher K. Nano-graphene oxide for cellular imaging and drug delivery. Nano Res 2008;1:203–12.
[9] Luo Z, Vora PM, Mele EJ, Johnson AC, Kikkawa JM. Photoluminescence and band gap modulation in graphene oxide. Appl Phys Lett 2009;94:111909.
[10] Liu X, Guo Y, Wang D, Yang X, Liu W, Qin W. Graphene oxide functionalization with aminocoumarin nanosheet fluorescent dye: preparation, electrochemistry, spectroscopy and imaging in the living cells. Dyes Pigments 2015;113:327–35.
[11] Mei Q, Zhang K, Guan G, Liu B, Wang S, Zhang Z. Highly efficient photoluminescent graphene oxide with tunable surface properties. Chem Commun 2010;46:7319–21.
[12] Kim J, Cote LJ, Kim F, Huang J. Visualizing graphene based sheets by fluorescence quenching microscopy. J Am Chem Soc 2010;132:260–7.
[13] Novoselov KS, Geim AK, Morozov SV, Jiang D, Zhang Y, Dubonos SV, Grigorieva IV, Firsov AA. Electric field effect in atomically thin carbon films. Science 2004;306:666–9.
[14] Hu R, Zhang X, Kong R, Zhao X, Jiang J, Tan W. Nucleic acid-functionalized nanomaterials for bioimaging applications. J Mater Chem 2011;21:16323–34.
[15] Lu C, Yang H, Zhu C, Chen X, Chen G. A graphene platform for sensing biomolecules. Angew Chem Int Ed 2009;48:4785–7.
[16] Chang H, Tang L, Wang Y, Jiang J, Li J. Graphene fluorescence resonance energy transfer aptasensor for the thrombin detection. Anal Chem 2010;82:2341–6.
[17] Wang L, Zhu J, Han L. Graphene-based aptamer logic gates and their application to multiplex detection. ACS Nano 2012;6:6659–66.
[18] Wen Y, Xing F, He S. A graphene-based fluorescent nanoprobe for silver(I) ions detection by using graphene oxide and a silver-specific oligonucleotide. Chem Commun 2010;46:2596–8.
[19] Pu Y, Zhu Z, Han D, Liu H, Liu J, Liao J, Zhang K, Tan W. Insulin-binding aptamer-conjugated graphene oxide for insulin detection. Analyst 2011;136:4138–40.
[20] Sheng L, Ren J, MiaoY, Wang J, Wang E. PVP-coated graphene oxide for selective determination of ochratoxin A via quenching fluorescence of free aptamer. Biosens Bioelectron 2011;26:3494–9.
[21] Wang Y, Li Z, Hu D, Lin C, Li J, Lin Y. Aptamer/graphene oxide nanocomplex for *in situ* molecular probing in living cells. J Am Chem Soc 2010;132:9274–6.
[22] Zhu Z, Yang R, You M, Zhang X, Wu Y, Tan W. Single-walled carbon nanotube as an effective quencher. Anal Bioanal Chem 2010;396:73–83.
[23] Monteiro-Riviere NA, Nemanich RJ, Inman AO, Wang YY, Riviere JE. Toxicol Lett 2005;155:377–84.
[24] Kostarelos K, Lacerda L, Pastorin G, WuW, Wieckowski S, Luangsivilay J, Godefroy S, Pantarotto D, Briand J-P, Muller S, Prato M, Bianco A. Cellular uptake of functionalized carbon nanotubes is independent of functional group and cell type. Nat Nanotechnol 2007;2:108–13.
[25] Chen H, Yu C, Jiang C, Zhang S, Liu B, Kong J. A novel near-infrared protein assay based on the dissolution and aggregation of aptamer-wrapped single-walled carbon nanotubes. Chem Commun 2009;33:5006–8.
[26] Yang R, Tang Z, Yan J, Kang H, Kim Y, Zhu Z, Tan W. Noncovalent assembly of carbon nanotubes and single-stranded DNA: an effective sensing platform for probing biomolecular interactions. Anal Chem 2008;80:7408–13.
[27] Ouyang X, Yu R, Jin J, Li J, Yang R, Tan W, Yuan J. New strategy for label-free and time-resolved luminescent assay of protein: conjugate Eu^{3+} complex and aptamer-wrapped carbon nanotubes. Anal Chem 2011;83:782–9.
[28] Yan L, Shi H, He X, Wang K, Tang J, Chen M, Ye X, Xu F, Lei Y. A versatile activatable fluorescence probing platform for cancer cells *in vitro* and *in vivo* based on self-assembled aptamer/carbon nanotube ensembles. Anal Chem 2014;86:9271–7.
[29] Zhu Z, Tang Z, Phillips JA, Yang R, Wang H, Tan W. Regulation of singlet oxygen generation using single-walled carbon nanotubes. J Am Chem Soc 2008;130:10856–7.
[30] Xu X, Ray R, Gu Y, Ploehn HJ, Gearheart L, Raker K, Scrivens WA. Electrophoretic analysis and purification of fluorescent single-walled carbon nanotube fragments. J Am Chem Soc 2004;126:1273–7.
[31] Sun Y, Zhou B, Lin Y, Wang W, Shiral Fernando KA, Pathak P, Meziani MJ, Harruff BA, Wang X, Wang H, Luo PG, Yang H, Kose ME, Chen B, Veca LM, Xie S-Y. Quantum-sized carbon dots for bright and colorful photoluminescence. J Am Chem Soc 2006;128:7756–7.
[32] Qian ZS, Shan XY, Chai LJ, Chen JR, Feng H. A fluorescent nanosensor based on graphene quantum dots-aptamer probe and graphene oxide platform for detection of lead (II) ion. Biosens Bioelectron 2015;68:225–31.

[33] Wang Y, Bao L, Liu Z, Pang D. Aptamer biosensor based on fluorescence resonance energy transfer from upconverting phosphors to carbon nanoparticles for thrombin detection in human plasma. Anal Chem 2011;83:8130–7.
[34] Zhang L, Cui P, Zhang B, Gao F. Aptamer-based turn-on detection of thrombin in biological fluids based on efficient phosphorescence energy transfer from Mn-doped ZnS quantum dots to carbon nanodots. Chem Eur J 2013;19:9242–50.
[35] Ma N, Jiang W, Li T, Zhang Z, Qi H, Yang M. Fluorescence aggregation assay for the protein biomarker mucin 1 using carbon dot-labeled antibodies and aptamers. Microchim Acta 2015;182:443–7.
[36] Li H, He X, Kang Z, Huang H, Liu Y, Liu J, Lian S, Tsang CHA, Yang X, Lee S-T. Water-soluble fluorescent carbon quantum dots and photocatalyst design. Angew Chem Int Ed 2010;49:4430–4.
[37] Ha HD, Jang M, Liu F, Cho Y, Seo TS. Upconversion photoluminescent metal ion sensors via two photon absorption in graphene oxide quantum dots. Carbon 2015;81;367–75.
[38] Liu J, Yu J, Chen J, Shih K. Noncovalent assembly of carbon nanoparticles and aptamer for sensitive detection of ATP. RSC Adv 2014;4:38199–205.
[39] Fan C, Wang S, Hong JW, Bazan GC, Plaxco KW, Heeger AJ. Beyond superquenching: hyper-efficient energy transfer from conjugated polymers to gold nanoparticles. Proc Natl Acad Sci USA 2003;100:6297–301.
[40] Zheng D, Seferos DS, Giljohann DA, Patel PC, Mirkin CA. Aptamer nano-flares for molecular detection in living cells. Nano Lett 2009;9:3258–61.
[41] Zhang J, Wang L, Zhang H, Boey F, Song S, Fan C. Aptamer-based multicolor fluorescent gold nanoprobes for multiplex detection in homogeneous solution. Small 2010;6:201–4.
[42] Chen Y, O'Donoghue MB, Huang Y, Kang H, Phillips JA, Chen X, Estevez M-C, Yang CJ, Tan W. A surface energy transfer nanoruler for measuring binding site distances on live cell surfaces. J Am Chem Soc 2010;132:16559–70.
[43] Lohse SE, Murphy CJ. The quest for shape control: a history of gold nanorod synthesis. Chem Mater 2013;25:1250–61.
[44] Wang J, You M, Zhu G, Shukoor MI, Chen Z, Zhao Z, Altman MB, Yuan Q, Zhu Z, Chen Y, Huang CZ, Tan W. Photosensitizer-gold nanorod composite for targeted multimodal therapy. Small 2013;9:3678–84.
[45] Yun CS, Javier A, Jennings T, Fisher M, Hira S, Peterson S, Hopkins B, Reich NO, Strouse GF. Nanometal surface energy transfer in optical rulers, breaking the FRET barrier. J Am Chem Soc 2005;127:3115–9.
[46] Dulkeith E, Ringler M, Klar TA, Feldmann J. Gold nanoparticles quench fluorescence by phase induced radiative rate suppression. Nano Lett 2005;5:585–9.
[47] Shang L, Dong S, Nienhaus GU. Ultra-small fluorescent metal nanoclusters: synthesis and biological applications. Nano Today 2011;6:401–18.
[48] Liu J, Yan C. Competitive aptamer bioassay for selective detection of adenosine triphosphate based on metal-paired molecular conformational switch and fluorescent gold nanoclusters. Biosens Bioelectron 2012;36:135–41.
[49] Li C, Chen T, Ocsoy I, Zhu G, Yasun E, You M, Wu C, Zheng J, Song E, Huang CZ, Tan W. Gold-coated Fe_3O_4 nanoroses with five unique functions for cancer cell targeting, imaging, and therapy. Adv Funct Mater 2014;24:1772–80.
[50] Levy M, Cater SF, Ellington AD. Quantum-dot aptamer beacons for the detection of proteins. ChemBioChem 2005;6:2163–6.
[51] Freeman R, Girsh J, Jou AF, Ho JA, Hug T, Dernedde J, Willner I. Optical aptasensors for the analysis of the vascular endothelial growth factor (VEGF). Anal Chem 2012;84:6192–8.
[52] Hu D, Zhang P, Gong P, Lian S, Lu Y, Gao D, Cai L. A fast synthesis of near-infrared emitting CdTe/CdSe quantum dots with small hydrodynamic diameter for *in vivo* imaging probes. Nanoscale 2011;3:4724–32.
[53] Liu J, Lee JH, Lu Y. Quantum dot encoding of aptamer-linked nanostructures for one-pot simultaneous detection of multiple analytes. Anal Chem 2007;79:4120–5.
[54] Zrazhevskiy P, Sena M, Gao X. Designing multifunctional quantum dots for bioimaging, detection, and drug delivery. Chem Soc Rev 2010;39:4326–54.
[55] Xu B, Zhao C, Wei W, Ren J, Miyoshi D, Sugimoto N, Qu X. Aptamer carbon nanodot sandwich used for fluorescent detection of protein. Analyst 2012;137:5483–6.
[56] Hou L, Zhu C, Wu X, Chen G, Tang D. Bioresponsive controlled release from mesoporous silica nanocontainers with glucometer readout. Chem Commun 2014;50;1441–43.
[57] Li L, Xie M, Wang J, Li X, Wang C, Yuan Q, Pang D-W, Lu Y, Tan W. A vitamin-responsive mesoporous nanocarrier with DNA aptamer-mediated cell targeting. Chem Commun 2013;49:5823–5.
[58] Zhang Z, Balogh D, Wang F, Sung SY, Nechushtai R, Willner I. Biocatalytic release of an anticancer drug from nucleic-acids-capped mesoporous SiO_2 using DNA or molecular biomarkers as triggering stimuli. ACS Nano 2013;7:8455–68.
[59] Tadjarodia A, Abbaszadeh A, Taghizadeh M, Shekari N, Asgharinezhad AA. Solid phase extraction of Cd(II) and Pb(II) ions based on a novel functionalized Fe_3O_4@SiO_2 core-shell nanoparticles with the aid of multivariate optimization methodology. Mater Sci Eng C 2015;49:416–21.
[60] Lai C, Hsiao Y, Peng Y, Chou P. Facile synthesis of highly emissive carbon dots from pyrolysis of glycerol; gram scale production of carbon dots/mSiO_2 for cell imaging and drug release. J Mater Chem 2012;22:14403–9.
[61] Zhang P, Cheng F, Zhou R, Cao J, Li J, Burda C, Min Q, Zhu J-J. DNA-hybrid-gated multifunctional mesoporous silica nanocarriers for dual-targeted and microRNA-responsive controlled drug delivery. Angew Chem Int Ed 2014;53:2371–5.
[62] Cao F, Deng R, Liu D, Song S, Wang S, Su S, Zhang H. Fabrication of fluorescent silica-Au hybrid nanostructures for targeted imaging of tumor cells. Dalton Trans 2011;40:4800–2.
[63] Babu E, Mareeswaran PM, Rajagopal S. Highly sensitive optical biosensor for thrombin based on structure switching aptamer-luminescent silica nanoparticles. J Fluoresc 2013;23:137–46.
[64] He X, Li Y, He D, Wang K, Shangguan J, Shi H. Aptamer-fluorescent silica nanoparticles bioconjugates based dual-color flow cytometry for specific detection of staphylococcus aureus. J Biomed Nanotechnol 2014;10:1359–68.
[65] Herr JK, Smith JE, Medley CD, Shangguan D, Tan W. Aptamer-conjugated nanoparticles for selective collection and detection of cancer cells. Anal Chem 2006;78:2918–24.
[66] Jo H, Her J, Ban C. Dual aptamer-functionalized silica nanoparticles for the highly sensitive detection of breast cancer. Biosens Bioelectron 2015;71:129–36.

[67] Li H, Mu Y, Lu J, Wei W, Wan Y, Liu S. Target-cell-specific fluorescence silica nanoprobes for imaging and theranostics of cancer cells. Anal Chem 2014;86:3602–9.
[68] Ding K, Alemdaroglu FE, Börsch M, Berger R, Herrmann A. Engineering the structural properties of DNA block copolymer micelles by molecular recognition. Angew Chem Int Ed 2007;46:1172–5.
[69] Wu Y, Sefah K, Liu H, Wang R, Tan W. DNA aptamer–micelle as an efficient detection/delivery vehicle toward cancer cells. Proc Natl Acad Sci USA 2010;107;5–10.
[70] Li X, Yu Y, Ji Q, Qiu L. Targeted delivery of anticancer drugs by aptamer AS1411 mediated Pluronic F127/cyclodextrin-linked polymer composite micelles. Nanomed Nanotechnol 2015;11:175–84.
[71] Zhang L, Lei J, Liu L, Li C, Ju H. Self-assembled DNA hydrogel as switchable material for aptamer-based fluorescent detection of protein. Anal Chem 2013;85:11077–82.
[72] Helwa Y, Dave N, Froidevaux R, Samadi A, Liu J. Aptamer-functionalized hydrogel microparticles for fast visual detection of mercury(II) and adenosine. ACS Appl Mater Interfaces 2012;4:2228–33.
[73] Lee JB, Peng S, Yang D, Roh YH, Funabashi H, Park N, Rice EJ, Chen L, Long R, Wu M, Luo D. A mechanical metamaterial made from a DNA hydrogel. Nat Nanotechnol 2012;7:816–20.
[74] Lee JB, Hong J, Bonner DK, Poon Z, Hammond PT. Self-assembled RNA interference microsponges for efficient siRNA delivery. Nat Mater 2012;11:316–22.
[75] Zhu G, Hu R, Zhao Z, Chen Z, Zhang X, Tan W. Noncanonical self-assembly of multifunctional DNA nanoflowers for biomedical applications. J Am Chem Soc 2013;135:16438–45.
[76] Hu R, Zhang X, Zhao Z, Zhu G, Chen T, Fu T, Tan W. DNA nanoflowers for multiplexed cellular imaging and traceable targeted drug delivery. Angew Chem Int Ed 2014;53:5821–6.
[77] Dirks RM, Pierce NA. Triggered amplification by hybridization chain reaction. Proc Natl Acad Sci USA 2004;101:152758.
[78] Xuan F, Hsing I. Triggering hairpin-free chain-branching growth of fluorescent DNA dendrimers for nonlinear hybridization chain reaction. J Am Chem Soc 2014;136:9810–3.
[79] Zhu G, Zheng J, Song E, Donovan M, Zhang K, Liu C, Tan W. Self-assembled, aptamer-tethered DNA nanotrains for targeted transport of molecular drugs in cancer theranostics. Proc Natl Acad Sci USA 2013;110:7998–8003.
[80] Zhu G, Zhang S, Song E, Zheng J, Hu R, Fang X, Tan W. Building fluorescent DNA nanodevices on target living cell surfaces. Angew Chem Int Ed 2013;52:5490–6.
[81] Rothemund PWK. Folding DNA to create nanoscale shapes and patterns. Nature 2006;440:297–302.
[82] Mitchell N, Schlapak R, Kastner M, Armitage D, Chrzanowski W, Riener J, Hinterdorfer P, Ebner A, Howorka S. A DNA nanostructure for the functional assembly of chemical groups with tunable stoichiometry and defined nanoscale geometry. Angew Chem Int Ed 2009;48:525–7.
[83] Zhang Y, Seeman NC. Construction of a DNA-truncated octahedron. J Am Chem Soc 1994;116:1661–9.
[84] Ke Y, Lindsay S, Chang Y, Liu Y, Yan H. Self-assembled water-soluble nucleic acid probe tiles for label-free RNA hybridization assays. Science 2008;319:180–3.
[85] Rinker S, Ke Y, Liu Y, Chhabra R, Yan H. Self-assembled DNA nanostructures for distance-dependent multivalent ligand-protein binding. Nat Nanotechnol 2008;3:418–22.
[86] Yuan Q, Lu D, Zhang X, Chen Z, Tan W. Aptamer-conjugated optical nanomaterials for bioanalysis. TrAC 2012;39:72–86.